An Evaluation of Evaporation over the Tropical Pacific Ocean as Observed from Satellites

YURIE HETA AND YASUSHI MITSUTA

Disaster Prevention Research Institute, Kyoto University, Kyoto, Japan

(Manuscript received 28 January 1992, in final form 24 December 1992)

ABSTRACT

Based on the precipitable water data provided by Scanning Multichannel Microwave Radiometer (SMMR), and wind data by Geostationary Meteorological Satellite (GMS) and Geostationary Operational Environment Satellite (GOES), the monthly averaged water vapor flux and flux divergence have been estimated over the equatorial Pacific area for July 1980.

The main flow pattern of water vapor transport is essentially the combination of meridional convergence and westward flow. The intertropical convergence zone (ITCZ) in the northern part of the equatorial Pacific around 10°N, is characterized by water vapor convergence, which indicates that precipitation exceeds evaporation. The largest convergence areas of about 500 mm month^{-1} are seen over the ITCZ.

Evaporation can be estimated from the water vapor convergence if precipitation data, such as island rainfall data, are available. Over the eastern Pacific, where rainfall is nearly zero, evaporation is about 150 mm month^{-1} averaged over 0°–20S, 170°–90W. While precipitation is obtained if evaporation can be estimated by an independent method. Precipitation of more than 400 mm month^{-1} is seen around the ITCZ by the use of evaporation by bulk method.

1. Introduction

Water vapor is the main energy source of tropical disturbances such as typhoons and moisture transport and its budget in the troposphere are important factors in understanding the tropical phenomena. Many attempts to observe the water budget in the tropics have been made in the recent international projects of the GARP (Global Atmosphere Research Program) Atlantic Tropical Experiment (GATE), First GARP Global Experiment (FGGE), etc. However, technical difficulties in observation have prevented obtaining reliable results in this wide area. A new attempt is planned by the Tropical Ocean Global Atmosphere (TOGA) program to make a direct measurement of turbulent flux of water vapor on the cruising ship, as proposed by Mitsuta and Fujitani (1974). However, it is still almost impossible to make such a direct measurement over the whole tropics.

The present study is another approach to the study of the water budget over the tropical Pacific Ocean in the synoptic scale. The water vapor transport is also obtained from satellite-borne precipitable water data. Worldwide distribution of the vertically integrated atmospheric columnar water vapor over the ocean has been obtained from the Scanning Multichannel Microwave Radiometer (SMMR) on board the *Nimbus-7* satellite on a 2° × 2° grid. The product of this precipitable water and the 850-hPa wind data representing the lower-tropospheric wind roughly expresses the water vapor transport, as shown in the next section. The synoptic-scale tropospheric water budget can be obtained from the relation that the horizontal divergence of water vapor transport in the troposphere is balanced by the difference of water vapor loss by rainfall and water supply from the ocean by evaporation. If rainfall data are obtained, evaporation will be estimated and vice versa.

In section 3, we show some trials to estimate evaporation or precipitation in this method. Evaporation is evaluated from water vapor convergence and island rainfall data. On the other hand precipitation is estimated from water vapor convergence and evaporation by the bulk method. Nowadays many attempts have been made to estimate precipitation or evaporation by using various kinds of satellite data. If we can obtain one of the pair of precipitation and evaporation, the other will be estimated from this subtraction.

2. Water vapor flux

In this section, the evaluation of water vapor transport by using vertically integrated atmospheric columnar water vapor data and lower-tropospheric wind data is explained. Distribution of precipitable water W based on the global monthly average in every 2° × 2° latitude–longitude mesh by W. Liu (1987) (as obtained by SMMR on *Nimbus-7* satellite for July in 1980) is shown in Fig. 1. Liu (1987) indicated that the precip-

Corresponding author address: Dr. Yurie Heta, Disaster Prevention Research Institute, Kyoto University, Gokasho, Uji, Kyoto, Japan, 611.

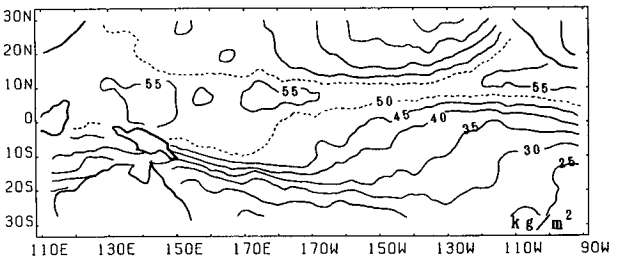

FIG. 1. Monthly averaged atmospheric columnar integrated water vapor measured by SMMR for July 1980. Contour interval is 5.0 kg m^{-2}.

itable water observed by satellite is in good agreement with the vertically integrated water vapor content by rawin observation over the tropical Pacific. The zone of high water vapor content extends along the 10°N zone in summer. Rich water vapor areas higher than 55 kg m^{-2} are seen around 5°N, 140°E; 10°N, 180°; and 12°N, 100°W in July 1980. In the eastern Pacific, precipitable water decreases rapidly toward north and south of the ITCZ, while the rich precipitable water area is latitudinally broad in the western Pacific.

Water vapor transport $\mathbf{Q}$ is calculated by vertical integration of the product between horizontal wind and water vapor at each altitude. However, since water vapor content essentially exists in the lower troposphere, water vapor transport can be estimated by using the integrated water vapor W and representative wind of the lower troposphere. Figure 2 shows the vertical distribution of water vapor for some stations in Japanese islands based on the data in *Aerological Data of Japan, July 1980* assimilated by the Japan Meteorological Agency (JMA). Water vapor rapidly decreases with height in the troposphere. The center of gravity of water vapor distribution is shown on the right-hand side of Fig. 2. The 850-hPa wind field is used as the representative wind at the lower troposphere study. If the satellite-observed ocean surface wind is given, more reliable representative wind fields will be obtained. However at the present, the 850-hPa wind field has the best accuracy over the ocean by the existence of the lower-cloud wind observed by satellites (Hamada 1982). Based on the GMS and GOES satellite wind data and rawinsonde data, the 850-hPa wind fields were assimilated daily by the mass consistent atmospheric flux (MASCON) model using the variational technique for July 1980 (Heta 1990, 1991). Monthly average of the wind fields for July 1980 in 2° × 2°, $\overline{\mathbf{V}_{850\,\mathrm{hPa}}}$, is used for this study.

The horizontal transport of water vapor can be estimated by the product of the total precipitable water and the 850-hPa wind vector, because the center of gravity of the water vapor distribution in the troposphere is located near the 850-hPa level shown as the representative height in Fig. 2. The profile of water vapor in the tropics shows a similar pattern as well. For the purpose of verification, the values of $\int_0^{z(300\,\mathrm{hPa})} \rho_{vz}\mathbf{V}_z dz$ and $\int_0^{z(300\,\mathrm{hPa})} \rho_{vz} dz \mathbf{V}_{850\,\mathrm{hPa}}$ are calculated for the same five islands shown in Fig. 2, where ρ_{vz} is the density of water vapor at the height of z. Comparing the values of $\int_0^{z(300\,\mathrm{hPa})} \rho_{vz}\mathbf{V}_z dz$ and $\int_0^{z(300\,\mathrm{hPa})} \rho_{vz} dz \mathbf{V}_{850\,\mathrm{hPa}}$, the latter value is about 20% larger on average than the former because of the change of wind directions between the upper and lower troposphere. However, the directions of total transport show almost same values for both expressions. Therefore the next assumption can be roughly accepted:

$$\mathbf{Q} = \overline{W\mathbf{V}_{850\,\mathrm{hPa}}}. \tag{1}$$

Moreover, Eq. (1) can be rewritten as the sum of the stationary term $\overline{W}\,\overline{\mathbf{V}_{850\,\mathrm{hPa}}}$ and the transient term $\overline{W'\mathbf{V}'_{850\,\mathrm{hPa}}}$ as follows:

$$\mathbf{Q} = \overline{W}\,\overline{\mathbf{V}_{850\,\mathrm{hPa}}} + \overline{W'\mathbf{V}'_{850\,\mathrm{hPa}}}. \tag{2}$$

However, as far as the long-term average (such as the monthly mean) is concerned, the transient term is much smaller than the stationary term. This is shown as follows; an inequity is gained by considering correlation between W and $\mathbf{V}_{850\,\mathrm{hPa}}$:

$$|\overline{W'\mathbf{V}'_{850\,\mathrm{hPa}}}| \leq \sigma_W \sigma_{\mathbf{V}_{850\,\mathrm{hPa}}}, \tag{3}$$

where σ means standard deviation. Estimating and comparing the value of the right-hand side of Eq. (3) and the absolute value of stationary term, $|\overline{W}\,\overline{\mathbf{V}_{850\,\mathrm{hPa}}}|$, the value of $\sigma_W \sigma_{\mathbf{V}_{850\,\mathrm{hPa}}}$ is less than 5% of the value of $|\overline{W}\,\overline{\mathbf{V}_{850\,\mathrm{hPa}}}|$. Therefore, the stationary term is considered to be the representative of the total water vapor flux. Chen (1985) has also shown the same result for the tropics.

The distribution of water vapor transport in the tropical Pacific in July 1980 is shown in Fig. 3, which is obtained from the mean precipitable water and 850-hPa wind by using the method shown above. The westward transport, due to the strong easterly winds, is dominant in the tropics. The largest westward transport is located around 10°N, 165°W during this month. The maximum magnitude of water vapor transport is above 400 kg m^{-1} s^{-1}. Over the eastern Pacific around 130W, southwestward transport from the north, and northwestward transport from the south are converging into the ITCZ zone along 10°N. On the other hand, over the western Pacific, the westward transport north of the equator decreases rapidly between the date line and 140°E, and northeastward flow of water vapor recurving from the northwestward flow in the Southern Hemisphere is converging to the main flow.

3. Estimation of the evaporation

The divergence of horizontal water vapor flux can be written as follows if the state is sufficiently stationary to neglect the transient term,

$$\nabla \cdot \mathbf{Q} \approx E - P, \tag{4}$$

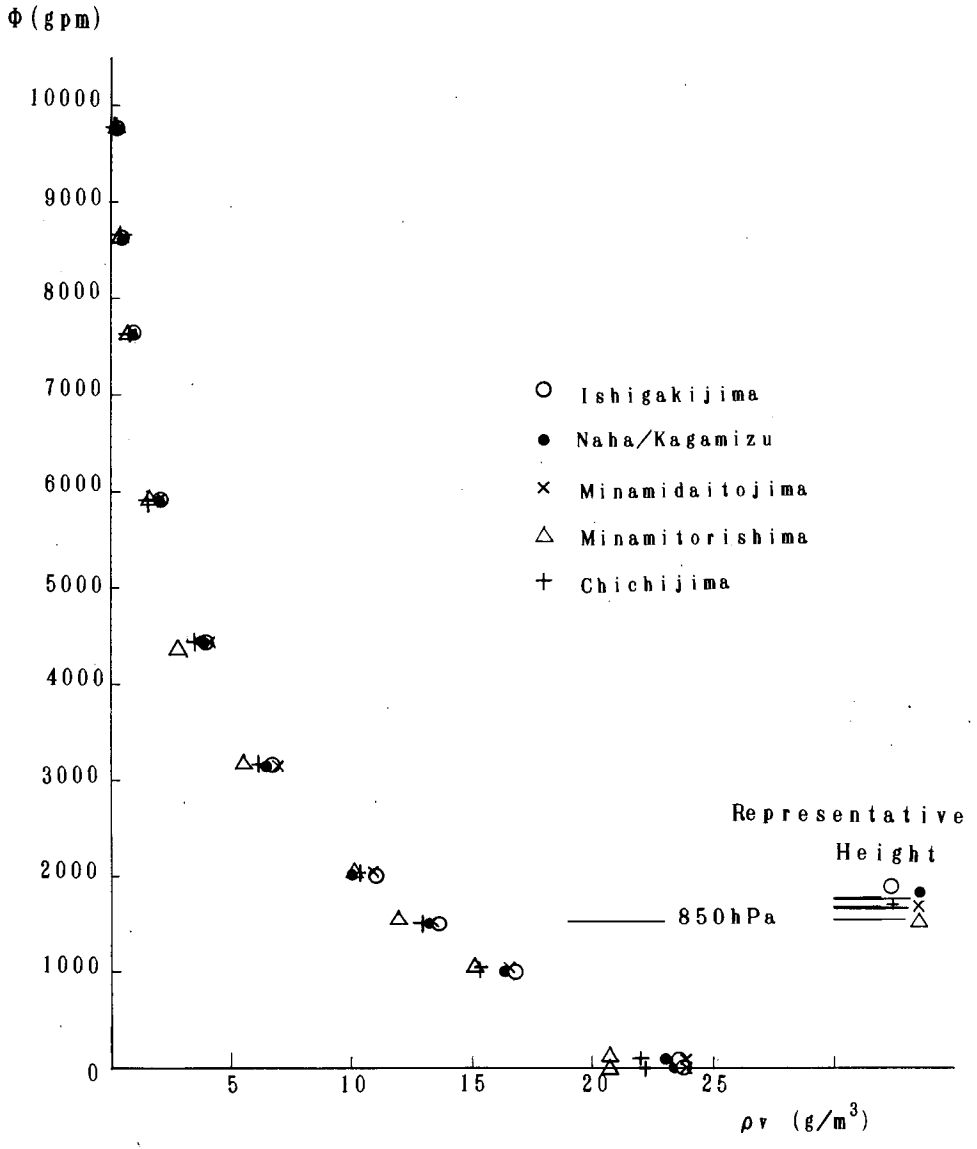

FIG. 2. The water vapor distribution in five Japanese islands. The location is shown in Table 1. The representative height shows the altitude of the center of gravity of the water vapor distribution in the troposphere.

where P is precipitation and E is evaporation. The water vapor flux divergence $\nabla \cdot \mathbf{Q}$ for July 1980 is shown in Fig. 4. In this figure the unit is 10^{-4} kg m^{-2} s^{-1}, which corresponds to a 268-mm water depth per month. North of the equator, there is a zone of high convergence of water vapor between 5° and 15°N, where precipitation exceeds evaporation or $(E - P < 0)$. The largest convergence value exceeds 3×10^{-4} kg m^{-2} s^{-1} (800 mm month^{-1}) over the equatorial Pacific. In the western Pacific, large convergence values of about 500 mm month^{-1} are scattered along the ITCZ. The divergence area extends zonally over the southeastern equatorial Pacific (0°–20°S) and the northern part of the central equatorial Pacific centered at 25°N, 155°W. The largest value of divergence in this region was about 2×10^{-4} kg m^{-2} s^{-1} (530 mm month^{-1}) in July 1980.

Integrating the water vapor divergence over the whole equatorial Pacific area (30°S–30°N, 110°E–94°W), excluding values over land, the total value over the whole region was -2.11×10^{15} kg month^{-1} in July 1980. This negative value indicates an excess of precipitation over evaporation. Therefore, the water vapor transported from outside the analyzed area fell down as rain over the whole area on average. The average rainfall excess over evaporation is 22 mm month^{-1}. Water vapor is mainly transported into the analyzed area in the equatorial Pacific from the eastern and the southern boundaries. The ocean around South and

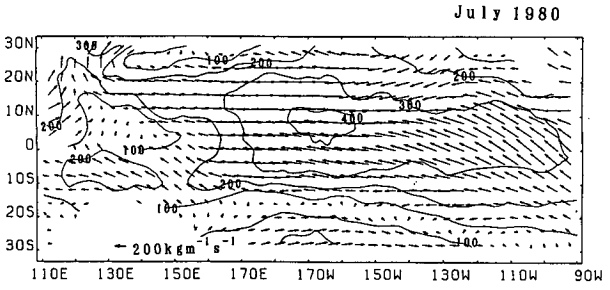

FIG. 3. Distribution of vertically integrated water vapor transport vector field for July 1980. Contour interval is 100 kg m^{-1} s^{-1}.

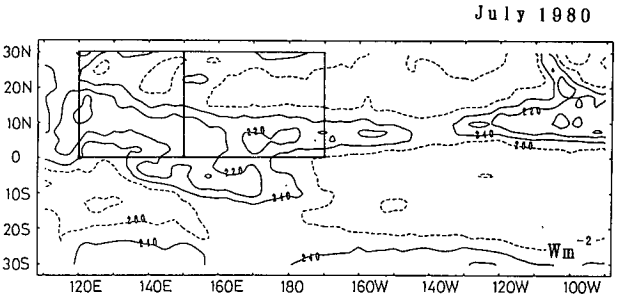

FIG. 5. Monthly averaged values of OLR from NOAA satellite for July 1980. Contour interval is 20 W m^{-2}. Two rectangles indicate the averaging domains for the profiles in Fig. 6.

North America supplies much water vapor to the Pacific atmosphere in the analyzed area.

Observation of precipitation over the ocean is sparse. Observed data for several islands from other papers are shown in Table 1 (Prabhakara et al. 1986). Japanese island data is also added to this table. The rainfall at Truk Island (7°28′N, 151°51′E) was 420 mm in July 1980. The water vapor flux divergence around this island, shown in Fig. 4, is -0.47×10^{-4} kg m^{-2} s^{-1} (-109 mm $month^{-1}$). Therefore, evaporation near this station can be estimated to be about 311 mm $month^{-1}$.

There are no stations over the southeastern Pacific, but we can roughly estimate the evaporation value because the precipitation is considered to be nearly zero as suggested in Fig. 5, which shows the distribution of outgoing longwave radiation (OLR) from a NOAA polar-orbiting satellite. The regions of low OLR values agree fairly well with the regions of strong convective motion in the midtroposphere in the tropics (Nakazawa 1986), and high values of OLR suggest negligibly small rainfall in the Southern Hemisphere. The southeastern tropical Pacific region (0°–20°S, 170° ~ 90°W), which shows the highest OLR values of 260 W m^{-2}, may be clear and the evaporation in this area is estimated to be about 150 mm $month^{-1}$. Along the 10°S zone, evaporation is estimated to be about 260 mm $month^{-1}$. It is interesting that the evaporation value over the southeastern tropical Pacific, where the SST is low, shows a large evaporation value; as high as along the ITCZ or the high-SST regions (Heta 1989).

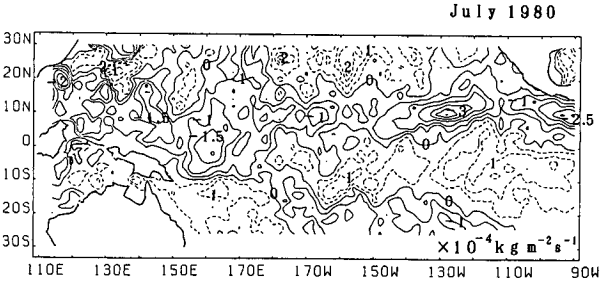

FIG. 4. Water vapor flux divergence $\nabla \cdot \mathbf{Q}$ (kg m^{-2} s^{-1}) for July 1980.

Liu (1988) estimated the latent heat flux with a bulk parameterization model for a few hundred bins in the northern part within 30°N–30°S, 110°E–70°W. The surface humidity is first derived from the precipitable water using a global empirical relation. The value of latent heat flux for July 1980 is about 120 W m^{-2}, while by ship it is about 135 W m^{-2} (Fig. 9 in Liu 1988). These values are about 130 and 145 mm $month^{-1}$, respectively. We get 20% or 30% larger values from rough estimation on trial by our method for the same area.

For checking our method, evaporation, E_b, is also estimated by the bulk method from the data of weather reports from commercial ships compiled by JMA, as the Marine Climatological Tables of the North Pacific Ocean for 1980. The evaporation E_b is evaluated from the latent heat flux LE as follows,

$$E_b = \frac{\mathrm{LE}}{L_v} = \rho C_E U (q_w - q), \tag{5}$$

where L_v is the latent heat of vaporization of water, ρ density of air, C_E water vapor transfer coefficient, U wind speed at the altitude of observation, and $q_w - q$ the difference of specific humidity between sea surface and air. The bulk transfer coefficient $C_E = 0.94 \times 10^{-3}$ obtained by direct measurement on the ship (Tsukamoto et al. 1990), is used in this calculation. The original data shown in the Marine Meteorological Tables are the monthly mean values of air temperature, dewpoint temperature, sea surface temperature (SST), atmospheric pressure, and so on, averaged over small rectangular sections of 2° in latitude and 5° in longitude. The method of calculation is similar to that of Mitsuta and Kato (1972). The values on each island are shown in Table 1. Comparing values of E and E_b, the values of E_b are narrower in the range between 131 and 206 mm $month^{-1}$, while the values of E are between 42 and 412 mm $month^{-1}$. The value of E at Truk is about 80% larger than that of E_b.

In general, Coral Island rainfall is assumed to be representative of open ocean rainfall (Kilonsky and Ramage 1976). However, in some cases, the precipi-

TABLE 1. Precipitation P, water vapor flux divergence $\nabla \cdot \mathbf{Q}$, and the estimated evaporation E and E_b. The values of the last row indicate the averages of values for eight Japanese islands.

Stations	Location	P	$\nabla \cdot \mathbf{Q}$	E	E_b
Truk	7°28′N, 151°51′E	420	−109	311	172
Ellice	8°31′S, 179°13′E	210	−24	186	—
Minamitorishima	24°18′N, 153°58′E	269	−131	138	140
Ishigakijima	24°20′N, 124°10′E	220	150	370	133
Yonagunijima	24°28′N, 123°01′E	49	70	119	133
Miyakojima	24°47′N, 125°17′E	133	174	307	206
Minamidaitojima	25°50′N, 131°14′E	195	−153	42	168
Naha/Kagamizu	26°12′N, 127°40′E	102	70	172	166
Kumejima	26°20′N, 126°48′E	112	300	412	166
Chichijima	27°05′N, 142°11′E	70	141	211	131
Average		143	78	221	155

tation data at an island is not the representative value over the small ocean area surrounding the island. Comparing rainfall on the Japanese islands and their adjacent ocean as estimated from satellite cloud data, Xie (1992) shows that the monthly rainfall over island is 50% larger than over the adjacent ocean. Considering this island effect, the evaporation E in Table 1 is probably biased toward high values. The average precipitation of eight Japanese islands in Table 1 is 143 mm month^{-1}. And water vapor flux divergence is 78 mm month^{-1}. The average evaporation is calculated 221 mm month^{-1} from Eq. (4); however, if the island effect of this amount is subtracted, the value of evaporation is about 170 mm month^{-1}.

Anyway, the accuracy of this estimation of evaporation depends on the representativeness of the rainfall data. Precipitation will be observed by radar on board the satellite in the near future in the Tropical Rainfall Measuring Mission (TRMM), and we will have more accurate values of evaporation as subtraction from water vapor flux convergence. Rainfall can also be estimated indirectly by the satellite cloud imagery (e.g., Arkin and Meisner 1987; Prabhakara et al. 1986; and so on). More reliable evaporation covering a wide area will be gained by use of such new rainfall data.

Conversely, precipitation P will be calculated if the evaporation can be obtained independently from Eq. (4). As a demonstration, we calculated P in this method from the evaporation by the bulk method, E_b over the northwestern Pacific (0°–30°N, 120°E–170°W) estimated at each grid of 2° latitude and 5° longitude as explained before. Figure 6 shows meridional distribution of E_b, $\nabla \cdot \mathbf{Q}$ and derived P averaged zonally in the western part (120°–150°E) and the eastern part

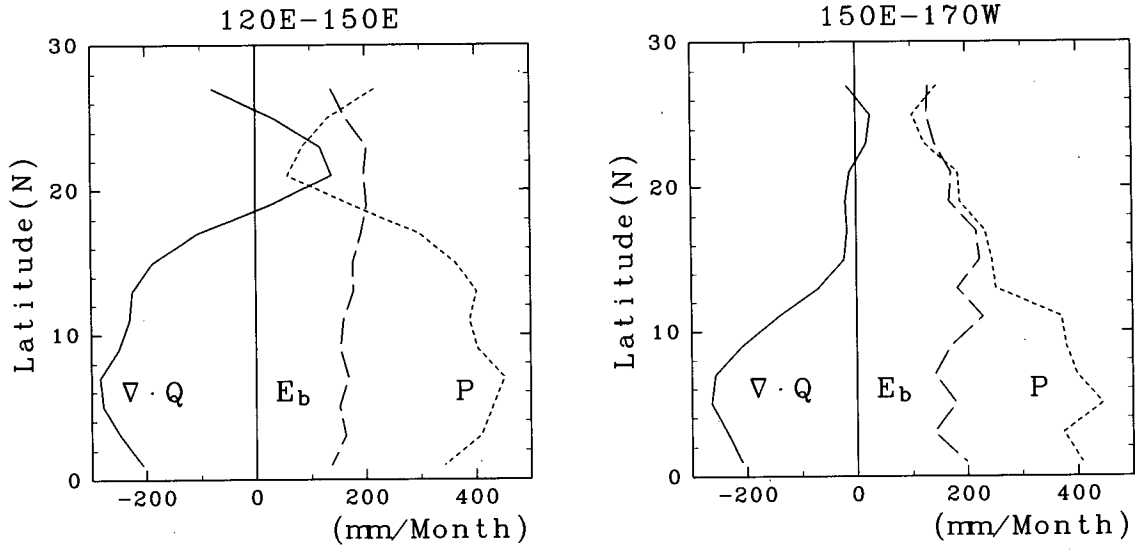

FIG. 6. Meridional distribution of the integrated water vapor flux divergence, precipitation, and evaporation, averaged zonally (a) between 120° and 150°E and (b) between 150°E and 170°W for July 1980; E_b is estimated by the bulk method and P is calculated from ($P = E_b - \nabla \cdot \mathbf{Q}$). The units are millimeters per month.

(150°E–170°W) of the equatorial Pacific as shown in Fig. 5. Precipitation is calculated as $E_b - \nabla \cdot \mathbf{Q}$ from Eq. (4). In the western region, $\nabla \cdot \mathbf{Q}$ shows smallest value, −284 mm month^{-1} at the 7°N zone, which means strong water vapor flux convergence. In the midlatitude zone centered at 21°N, water vapor flux divergence shows positive value. The estimated precipitation in this zone is only 58 mm month^{-1} in relation to positive flux divergence. The value of E_b shows moderate distribution and the average is 170 mm month^{-1}. The estimated precipitation exceeds 400 mm month^{-1} in the broad zone around the ITCZ in Fig. 6a. The rainfall at Truk is 420 mm month^{-1} in this month and this value agrees well with this estimated precipitation. Comparing the western and eastern areas (Figs. 6a and 6b), the high-precipitation area, where large water vapor convergence is recognized, extends more broadly north in the western region than the eastern region. This is coincident with the distributions of W in Fig. 1 and low-OLR values in Fig. 5. Although the periods are different, the values and distributions of precipitation quite agree with other estimated rainfall by Prabhakara et al. (1986), Janowiak and Arkin (1991), and others.

4. Conclusions

We have attempted to estimate the amount of water vapor flux and flux divergence over the equatorial Pacific Ocean by using the precipitable water data from the satellite. Roughly speaking, water vapor is transported from the Southern Hemisphere and the midlatitude of the northeastern Pacific to the cloud belt of the ITCZ, that is, from the low precipitable water area to the high water vapor area by the Hadley circulation against the gradient.

There are water vapor convergence areas along the ITCZ. The value of the water vapor convergence is about 500 mm month^{-1} in these areas, which represents the effective rainfall ($P - E$). Based on Japanese island rainfall data, the evaporation around 25°N in the western Pacific is estimated about 170 mm month^{-1}, taking into account the island effect. We can estimate the value of evaporation to be 150 mm month^{-1} over the Southern Hemisphere, where the rainfall is negligible. The evaporation is as high in the ITCZ as seen over the clear low-SST area in southeastern equatorial Pacific. If proper precipitation data exist, we will obtain more accurate evaporation value as the sum of water vapor flux divergence and precipitation. This is verified by the fact that the values of precipitation, conversely estimated by using evaporation values by the bulk method, are consistent with the cloud distribution and island data.

If precipitation data become available from TRMM, we can easily study water budget over the ocean surface from satellite data alone using the method shown in this paper.

Acknowledgments. We would like to thank Dr. T. Liu for providing *Nimbus-7* SMMR water vapor data. We wish to thank Dr. Nakazawa of the Meteorological Research Institute for providing NOAA OLR data. Thanks are due to Professor Y. K. Sasaki for his helpful comments and suggestions.

REFERENCES

Arkin, P. A., and B. N. Meisner, 1987: The relation between large-scale convective rainfall and cloud cover over western hemisphere during 1982–1984. *Mon. Wea. Rev.*, **115,** 51–74.

Chen, T.-C., 1985: Global water vapor flux and maintenance during FGGE. *Mon. Wea. Rev.*, **113,** 1801–1819.

Hamada, T., 1982: Representative heights of GMS satellite winds. Meteor. Satellite Center Tech. Note, **6,** 35–47.

Heta, Y., 1989: An analysis of water vapor transport over the Equatorial Pacific as observed from satellite. *Proc. International Symposium on Japanese Pacific Climate Study (JAPACS),* Tsukuba, Japan, Science and Technology Agency, 119–124.

——, 1990: An analysis of tropical wind fields in relation to typhoon formation over the western Pacific. *J. Meteor. Soc. Japan,* **68,** 65–77.

——, 1991: Origin of tropical disturbances in the equatorial Pacific. *J. Meteor. Soc. Japan,* **69,** 337–351.

Janowiak, J. E., and P. A. Arkin, 1991: Rainfall variations in the tropics during 1986–1989, as estimated from observations of cloud-top temperature. *J. Geophys. Res.*, **96,** 3359–3373.

Japan Meteorological Agency, 1980: *Aerological Data of Japan,* Japan Meteorological Agency, 252 pp.

Kilonsky, B. J., and C. S. Ramage, 1976: A technique for estimating tropical open-ocean rainfall from satellite observations. *J. Appl. Meteor.*, **15,** 972–975.

Liu, W. T., 1987: El Niño atlas, *Nimbus-7* microwave radiometer data. JPL Publication 87-5, Jet Propulsion Laboratory, 68 pp.

——, 1988: Moisture and latent heat flux variabilities in the tropical Pacific derived from satellite data. *J. Geophys. Res.*, **93,** 6749–6759.

Mitsuta, Y., and A. Kato, 1972: Climatological studies on air–sea interaction over the northwestern Pacific. *Bull. Disas. Prev. Res. Inst., Kyoto Univ.*, **22,** 37–51.

——, and T. Fujitani, 1974: Direct measurement of turbulent fluxes on a cruising ship. *Bound.-Layer Meteor.*, **6,** 203–217.

Nakazawa, T., 1986: Intraseasonal variations of OLR in the tropics during the FGGE year. *J. Meteor. Soc. Japan,* **64,** 17–34.

Prabhakara, C., D. A. Short, W. Wiscombe, R. S. Fraser, and B. E. Vollmer, 1986: Rainfall over oceans inferred from Nimbus 7 SMMR: Application to 1982–1983 El Niño. *J. Climate Appl. Meteor.*, **25,** 1464–1474.

Tsukamoto, O., E. Ohtaki, H. Ishida, M. Horiguchi, and Y. Mitsuta, 1990: On-board direct measurements of turbulent fluxes over the open sea. *J. Meteor. Soc. Japan,* **68,** 203–211.

Xie, P., 1992: Comparison of rainfall on the Japanese Islands and their adjacent ocean. *Bull. Disas. Prev. Res. Inst., Kyoto Univ.*, **42,** 19–30.